

Rigid-rod Langmuir-Blodgett films from [n]staffane-3-carboxylates

Huey C. Yang, Thomas F. Magnera, Chongmok Lee, Allen J. Bard, and Josef Michl

Langmuir, 1992, 8 (11), 2740-2746 • DOI: 10.1021/la00047a026

Downloaded from <http://pubs.acs.org> on January 23, 2009

More About This Article

The permalink <http://dx.doi.org/10.1021/la00047a026> provides access to:

- Links to articles and content related to this article
- Copyright permission to reproduce figures and/or text from this article



Rigid-Rod Langmuir-Blodgett Films from [n]Staffane-3-carboxylates

Huey C. Yang,^{1a} Thomas F. Magnera,^{1b} Chongmok Lee,^{1a,c} Allen J. Bard,^{1a} and Josef Michl^{*,1b}

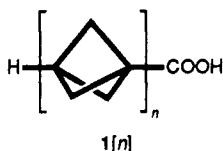
Department of Chemistry and Biochemistry, University of Colorado, Boulder, Colorado 80309-0215, and Department of Chemistry, University of Texas at Austin, Austin, Texas 78712-1167

Received June 22, 1992

The rigid-rod surfactants [n]staffane-3-carboxylates (1[n]) readily form Langmuir-Blodgett films when $n = 4$ and, with some effort, also when $n = 3$. The area per molecule, extrapolated to zero pressure, is nearly independent of the counterion ($26.0 \text{ \AA}^2/\text{molecule}$). Bilayer thickness in a multilayer assembly is $25.8 \pm 0.1 \text{ \AA}$ for Ca^{2+} 1[3], $32.2 \pm 0.1 \text{ \AA}$ for Ca^{2+} 1[4], and $31.4 \pm 0.1 \text{ \AA}$ for Cd^{2+} as determined by low-angle X-ray reflection. Ellipsometry yields the values 27.2 ± 1.0 , 33.2 ± 1.0 , and $32.6 \pm 1.0 \text{ \AA}$, respectively. The average tilt angle deduced from the difference between 1[3] and 1[4] is $17 \pm 5^\circ$. Independent IR measurements at normal incidence on Ge and grazing angle incidence on Au substrate yield the values $28 \pm 2^\circ$ and $19 \pm 2^\circ$, respectively. Only IR measurements were possible for a monolayer. They yielded the value $27 \pm 2^\circ$ at normal incidence on Ge and a distinctly different result at grazing incidence on Au, $0-10^\circ$. The larger average tilt values on the Ge surface are attributed to surface roughness.

The recent surge of interest in Langmuir-Blodgett (L-B) multilayer structures² has been driven at least in part by the promise that these materials hold for supramolecular engineering^{3,4} in areas such as nonlinear optics,⁵ pyroelectrics,⁶ and electron transfer studies.⁷ The salts of fatty acids, the usual construction materials for the films, are less than ideal for many of these applications. This is due at least in part to the floppy nature of the aliphatic chain, and it would be useful to find alternative L-B materials that have the form of rigid rods.

We have recently published the synthesis of [n]staffane-3-carboxylic acids 1[n], linear rigid-rod analogs of fatty acids.^{8,9} We now report that these materials form Langmuir-Blodgett films readily and provide an initial characterization of their structure.



Experimental Part

Samples. The preparation and purification of 1[3] and 1[4] have been reported.⁹

Area-Pressure Isotherms. Standard procedures² were followed, using a Model P Lauda preparative film balance (Brinkman Instruments). The acid 1[3] was introduced in chloroform solution (1 g/L), and 1[4] in a 4:1 chloroform-acetonitrile mixture (0.5 g/L). Before compression, the solvent

was allowed to evaporate for 15 min. A base line was checked to make sure that no excess solvent remained. Counterion effects were investigated by adding inorganic salts to the aqueous subphase to yield cation concentrations of $3 \times 10^{-4} \text{ M}$. A 0.5 M NaOH solution was added to adjust the pH to 7.0 ± 0.3 (i.e., the subphase solutions were unbuffered). Measurements on 1[3] were only possible when its solubility was decreased by saturating the aqueous layer with CaCl_2 (pH = 8.3). The isotherm of cadmium arachidate was measured as a standard.

Film Transfer. The films were transferred to a flat solid substrate by withdrawal or immersion under a constant pressure of 25 mN/m at a subphase temperature of $22.0 \pm 0.5^\circ \text{C}$. Silicon wafers polished on one side [N(100), Aurel Co.] served as substrates for ellipsometry ($50 \times 8 \times 0.2 \text{ mm}$) and low-angle X-ray reflection ($30 \times 15 \times 0.2 \text{ mm}$). They were ultrasonicated in chloroform twice for 10 min and treated with a very dilute solution of octadecyltrichlorosilane in chloroform to create a hydrophobic surface. Germanium ($30 \times 15 \times 2 \text{ mm}$) was used as a solid substrate for normal incidence IR transmission measurements (Wilmad Glass Co.). It was cleaned by dipping into chromic acid for a few seconds and rinsed with a copious amount of water. Glass microscope slides ($40 \times 25 \times 1 \text{ mm}$) with a 1500-Å layer of sputtered gold were used as substrates for grazing incidence IR reflection measurements. Just before film deposition, the IR substrates were briefly rinsed with a chromic acid solution and then washed with an excess of Millipore water (18 MΩ) to produce a hydrophilic surface. Y-type deposition¹⁰ was observed on all of the substrates; i.e., layers were deposited on both the dipping and the withdrawing stroke. The transfer ratio was 0.92-1.10.

Measurements. Ellipsometric measurements were performed using a Rudolph Model 437 ellipsometer (Rudolph Research, Flanders, NJ) equipped with a Model RR2000 automatic rotating analyzer and interfaced to a Hewlett-Packard Model 9816 desktop computer. Several strips of 2n layers ($n = 0-6$) were deposited next to each other on a single silicon substrate. Measurements were performed at 632.8 nm (He-Ne laser) and at an incidence angle of 70° . Data were expressed in terms of the conventional ellipsometric parameters¹¹ as $\delta\Delta = \Delta - \Delta_0$ and $\delta\psi = \psi - \psi_0$, where Δ_0 and ψ_0 refer to the bare substrate.

Low-angle X-ray reflection patterns of the L-B films were obtained on an assembly of seven bilayers using an automated Model APO 3520 Phillips powder diffractometer fitted with a

(1) (a) University of Texas. (b) University of Colorado. (c) Present address: Ewha Womans University, Seoul 120-750, Korea.

(2) Petty, M. C.; Barlow, W. A. In *Langmuir Blodgett Films*, Roberts, G., Ed.; Plenum Press: New York, 1990; Chapter 3.

(3) Kuhn, H. *Thin Solid Films* 1989, 178, 1.

(4) Barraud, A. *Thin Solid Films* 1989, 175, 73.

(5) Williams, D. J. *Angew. Chem., Int. Ed. Engl.* 1984, 23, 690.

(6) Davies, G. H.; Yarwood, J.; Petty, H. C.; Jones, C. A. *Thin Solid Films* 1988, 159, 461.

(7) Kuhn, H. J. *Photochem.* 1979, 10, 111. Möbius, D. *Acc. Chem. Res.* 1981, 14, 63. Kuhn, H. *Proceedings of the Robert A. Welch Foundation, Advances in Electrochemistry*; Robert A. Welch Foundation: Houston, TX, 1986; p 339. Polymeropoulos, E. E.; Möbius, D.; Kuhn, H. J. *Chem. Phys.* 1978, 68, 3918.

(8) Kaszynski, P.; Michl, J. *J. Am. Chem. Soc.* 1988, 110, 5225.

(9) Kaszynski, P.; Friedli, A. C.; Michl, J. *J. Am. Chem. Soc.* 1992, 114, 601.

(10) Blodgett, K. B. *J. Am. Chem. Soc.* 1935, 57, 1007.

(11) Azzam, R. M. A.; Bashara, N. M. *Ellipsometry and Polarized Light*; North-Holland: Amsterdam, 1977.

diffracted beam graphite monochromator and a theta compensating slit ($\text{Cu K}\alpha = 1.54178 \text{ \AA}$). This arrangement permitted diffraction lines to be measured down to about $2\theta = 1^\circ$, with a precision of about $\pm 0.02^\circ$. The program written for data analysis directly calculates the electron density distribution of the multilayer systems following the basic method of Hosemann and Bagchi¹² to obtain the total Patterson function and the deconvolution method of Pape¹³ to obtain the Patterson function of one unit cell.

Infrared measurements were performed on a Nicolet Model 60SX Fourier transform instrument with a HgCdTe detector cooled with liquid nitrogen and a wire grid polarizer (IGP225, Cambridge Physical Science), using 2000 scans and a resolution of 2 cm^{-1} . A Harrick Model RMA-00G reflection attachment was used for reflection measurements, using an incidence angle of 84° . Isotropic spectra were measured in a KBr pellet.

Results and Discussion

Our initial objective was to find out which, if any, $[n]$ -staffane-3-carboxylic acids ($1[n]$) and salts form L-B films. We found that the first three acids ($n = 1-3$) are too soluble in water to form such films. However, $1[3]$ will form a film on a concentrated aqueous solution of CaCl_2 , and this film has been transferred successfully to various solid substrates. The fourth member of the series, $1[4]$, has optimal properties and forms films readily on pure water, and these transfer well. No deterioration with time was observed. The fifth acid, $1[5]$, was found to be too insoluble in all organic spreading solvents tested, and we have not been able to use the standard techniques to make an L-B film of it.

Once it was established that $1[4]$, and to a lesser degree, $1[3]$, are suitable for the formation of L-B films, we became interested in characterizing their internal structure. While a thorough characterization of a two-dimensional structure requires a fair investment of effort, an initial survey of film thickness and determination of the rod tilt angle can be performed relatively simply. We have used ellipsometry, low-angle X-ray reflection, and IR spectroscopy for this purpose. While the first two methods are absolute, the sensitivity offered by the instrumentation accessible to us is such that only multilayers can be investigated. IR spectroscopy requires independent knowledge of IR transition moment directions in $1[n]$, which we have obtained in a separate investigation,¹⁴ and the FTIR spectrometer available to us had sufficient sensitivity to record reliable spectra even for a monolayer. The results revealed an interesting difference in the packing of a monolayer and a multilayer, and a future detailed two-dimensional structural investigation appears warranted.

Isotherms. The films were characterized by pressure-area isotherms. These were measured for $1[4]$ with a series of counterions (Figure 1) and for $1[3]$ with Ca^{2+} counterion (Figure 2). The course of all of the isotherms is very similar and consists of a gently rising part ("two-dimensional liquid") and a steeply rising part ("two-dimensional solid"). The near identity of the curves for $1[3]$ and $1[4]$ strongly suggests that these molecules pack in the same manner.

The "liquid" part of the isotherm is far more pronounced for $1[n]$ than it is for the standard L-B material, cadmium arachidate, shown in Figure 2 for comparison. Linear extrapolation of the steeply rising part to zero pressure yields exactly the same limiting area for $1[3]$ and $1[4]$, $26.0 \text{ \AA}^2/\text{molecule}$, essentially independent of the nature of

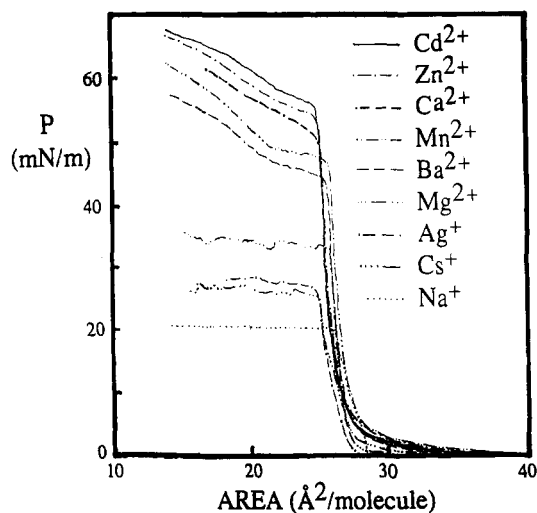


Figure 1. Room temperature isotherms for $[4]$ staffane-3-carboxylates with various counterions.

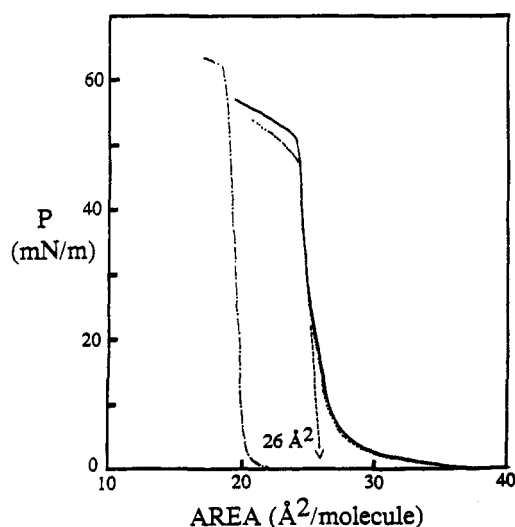


Figure 2. Room temperature isotherms for $\text{Ca}-[n]$ staffane-3-carboxylates with $n = 3$ (dotted line) and $n = 4$ (solid line). Cadmium arachidate (dot-dash line) is shown as a reference.

the counterion. Film collapse occurs at about 45 mN/m for $1[3]$ and 50 mN/m for $1[4]$, at $24.5 \text{ \AA}^2/\text{molecule}$.

The "zero-pressure" extrapolated area per molecule, $26.0 \text{ \AA}^2/\text{molecule}$, and the area of molecule at the point of collapse, $24.5 \text{ \AA}^2/\text{molecule}$, are both significantly larger than the corresponding numbers that we obtain for cadmium arachidate, 20 (reported¹⁵ $19-21 \text{ \AA}^2/\text{molecule}$) and $18 \text{ \AA}^2/\text{molecule}$, respectively. This result is compatible with the bulkier shape of the cylindrical $[n]$ staffane rod compared with an n -alkane chain, known from the simple crystal X-ray structures of the parent hydrocarbons, $[3]$ -staffane and $[4]$ staffane,¹⁶ and of many derivatives.¹⁷ The packing in the single crystals of the hydrocarbons is of the herring-bone type, with the molecular axes tilted at 21° ($[3]$ staffane) or 20° ($[4]$ staffane) from the crystal axis. The $[n]$ staffane rods mesh so that the bulging cages of one rod snuggle against the narrower waists between the cages on a neighboring rod. The repeat distance between the cages within a rod is 3.34 \AA , and the separation of the parallel axes on the closest neighbors is 5.36 \AA .

(12) Hosemann, R.; Bagchi, S. N. *Direct Analysis of Diffraction by Matter*; North-Holland: Amsterdam, 1962.

(13) Pape, E. H. *Biophys. J.* 1974, 14, 284.

(14) Murthy, G. S.; Hamrock, S. J.; Balaji, V.; Michl, J. *J. Phys. Chem.*, in press.

(15) Gaines, G. L., Jr. *Insoluble Monolayers at Liquid-Gas Interfaces*; John Wiley and Sons: New York, 1966.

(16) Murthy, G. S.; Hassenrück, K.; Lynch, V. M.; Michl, J. *J. Am. Chem. Soc.* 1989, 111, 7262.

(17) Friedli, A. C.; Lynch, V. M.; Kaszynski, P.; Michl, J. *Acta Crystallogr., Sect. B* 1990, 46, 377.

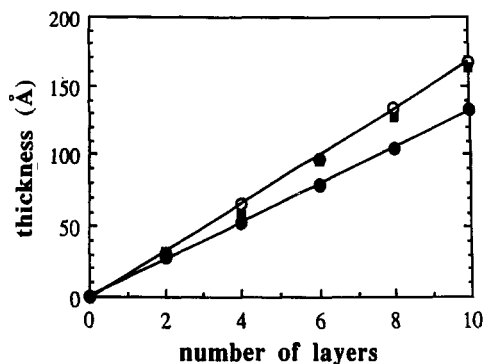


Figure 3. Ellipsometric film thickness vs number of layers from Ca-[3]staffane-3-carboxylate (solid circles), Ca-[4]staffane-3-carboxylate (open circles), and Cd-[4]staffane-3-carboxylate (hatched squares).

If the $[n]$ staffane cores of the molecules in our film were perpendicular to the water surface, such meshing would result in a radius of only 2.68 Å. Half of the molecules would have to be 1.67 Å further from the surface than the other half, but the projection of each molecule on the water surface would be close to a circle merely 22.6 Å² in area. The actual surface area per molecule in the compressed film would then depend on the nature of the two-dimensional packing. For instance, in a square lattice, which permits perfect neighbor meshing, it would be 28.8 Å².

Some meshing clearly occurs, since in its absence, with all molecules equidistant from the surface, the perpendicular orientation would cause each molecule to project a near circle with an area of 32.7 Å² as estimated using standard van der Waals radii. This is significantly in excess of the measured value. However, the meshing can be achieved by keeping the molecules equidistant from the surface and tilting them $\sim 20^\circ$ from the normal, as they are in the hydrocarbon crystal. This yields an area of 28.2 Å²/molecule.

While the measured area per molecule alone clearly will not permit us to deduce the molecular packing arrangement, its magnitude lies comfortably within reach of the above packing schemes and others that can be readily envisaged.

Additional information on the packing can be obtained from independent knowledge of the tilt angle. We have sought to determine this in two ways: (i) from the knowledge of the change of the metal ion to metal ion repeat distance upon going from 1[3] to 1[4], i.e., extending the length of the staffane rod pair by 6.68 Å; (ii) from band intensities in IR spectra.

Ellipsometry. A plot of $-\delta\Delta$ against longitudinal position of a sample covered with a series of strips revealed a regular series of steps corresponding to the increasing number of layer pairs deposited. The data points in the plateau regions were averaged. The fit of the $\delta\psi$ versus $\delta\Delta$ growth curve to theory was best when the refractive index of the film was assumed to be $n_f = 1.65 - 0.00i$. The standard value, $n_s = 3.84 - 0.12i$, was used for the silicon substrate. The value of n_f is higher than the usual $n_f \approx 1.50$ for fatty acids, but this is in line with the higher density of $[n]$ staffane derivatives.^{16,17}

A linear plot resulted for film thickness versus the number of layers (Figure 3). Results for average thickness of a pair of layers derived from these measurements are 27.2 ± 1.0 Å for Ca²⁺ 1[3], 33.2 ± 1.0 Å for Ca²⁺ 1[4], and 32.6 ± 1.0 Å for Cd²⁺ 1[4]. Much of the ± 1.0 Å uncertainty in the results originates in factors such as the assumed refractive index and affects results for 1[3] and 1[4] in the

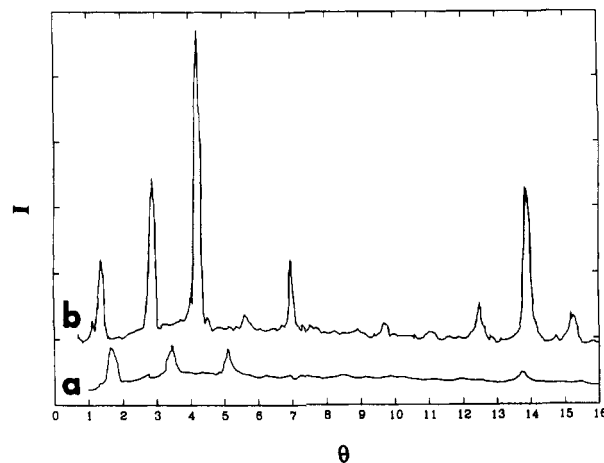


Figure 4. Low-angle X-ray reflection intensity vs angle for L-B films of Ca-[n]staffane-3-carboxylates, (a) $n = 3$ and (b) $n = 4$. The substrate background has been subtracted.

same direction. We estimate their difference to be 6.0 ± 0.5 Å, somewhat less than the 6.68 Å expected in the absence of tilt. If the packing of 1[3] and 1[4] is indeed the same, this yields an average tilt angle of $13\text{--}35^\circ$ for the Ca²⁺ films.

Low-Angle X-ray Reflection. Figure 4 shows low-angle X-ray reflection intensity recorded for the assemblies of seven bilayers of LB films of Ca²⁺ 1[n], $n = 3$ and 4. The film exhibits high order. Literature procedures¹⁸ were used to correct the peak intensities for all specimens for a $\sin \theta$ intensity variation due to the theta-compensating slit system and for polarization effects.¹⁹ Peak separations yield repeat distances between Ca²⁺ ion layers as 25.8 ± 0.1 Å and 32.2 ± 0.1 Å for 1[3] and 1[4], respectively, i.e., an increase by 6.4 ± 0.14 Å upon a 6.68-Å increase in the length of a rod pair. This yields an average tilt angle of $12\text{--}21^\circ$.

Analysis of peak intensities yields the electron density distribution in the unit cell of the Ca²⁺ 1[3] and 1[4] multilayers (Figure 5). The electron density curves are subject to the usual¹⁸ truncation artifact which appears as a deep second well after the metal cation peak at the graph edge, and they have a finite resolution of only 1.5 Å. Both of these limitations are dictated by the finite number of observed Bragg reflections.

Within these constraints, it is still possible to interpret three features of the density graph: (i) the high electron density associated with the Ca²⁺ ion at the top and the bottom of the unit cell; (ii) the very low electron density associated with the plane of van der Waals H \cdots H contacts in the center of the unit cell; (iii) an intermediate region of oscillating electron density. The peaks located in this region are presumed to correspond to the methylene carbons of the bicyclo[1.1.1]pentane cages in the staffane, and the troughs to the intercage C-C bonds. Although the available resolution does not permit us to use the observed separations between peaks to determine the packing geometry, its size clearly is of the right order of magnitude, about 3–3.5 Å. The amplitude of the oscillations is determined by the intensities of the Bragg peaks of orders 8, 9, and 9–11 in the case of 1[3] and 1[4], respectively. The lower amplitudes observed for 1[3] indicate a lower degree of ordering in this multilayer, and this is probably associated with the presence of a saturated CaCl₂ solution during the deposition process. The failure of the electron density to drop to values as low as observed

(18) Lesslauer, W.; Blasie, J. K. *Biophys. J.* 1972, 12, 175.

(19) Blaurock, A. E.; Worthington, C. R. *Biophys. J.* 1966, 6, 305.

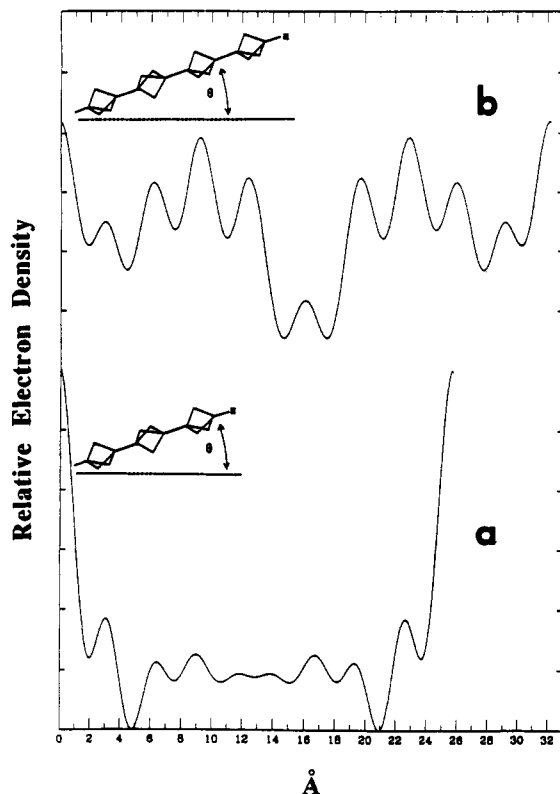


Figure 5. Projection of the relative unit cell electron densities in L-B films of Ca-[*n*]staffane-3-carboxylates, (a) *n* = 3 and (b) *n* = 4, onto the surface normal. The vertical scale is arbitrary.

for 1[4] in the region of the H...H interactions suggests that this region may contain occlusions of a saturated salt solution.

The unsubstituted terminal cages of the rods are well separated across the hydrophobic contact plane. Using a tilt angle of 17°, C-H bond length of 1.06 Å, and a 1.2 Å van der Waals radius for H, we would expect a maximum separation of 6.2 Å. The observed separation is 6.8 in 1[3] and 7.5 Å in 1[4], suggesting that some water may be occluded between the layers of 1[*n*].

In contrast, the carboxylate-carrying terminal cages lying across the ionic contact plane are rather close to each other: 6.4 Å in 1[3] and 5.8 Å in 1[4]. It is hard to say just what distance to expect from the covalent and ionic radii in the absence of detailed packing information, but it is clear that the anions and cations are meshed and nearly in the same plane, as proposed for manganese stearate.²⁰

For 1[4], the measurement was repeated with Cd²⁺ as the counterion (Figure 6). The Cd²⁺-Cd²⁺ layer separation was 31.4 ± 0.1 Å. Up to 17 reflection peaks were observed in this case, and these films appeared to be of superior quality. The electron density distribution is shown in Figure 7. The electron density at the metal is now much higher than for the calcium-containing film and dominates the X-ray diffraction at low orders. Nevertheless, the variation in electron density along the staffane rods is still clearly apparent and contributes conspicuous intensity to diffraction orders 9 and 10. The packing is clearly different from that deduced for the calcium salt, in that the unsubstituted terminal cages of the rods now are only about 4.5 Å apart, and these ends must be interdigitated.

The discrepancies between the bilayer thickness values derived from ellipsometry and those derived from X-ray reflection are disturbing. The systematic underestimation

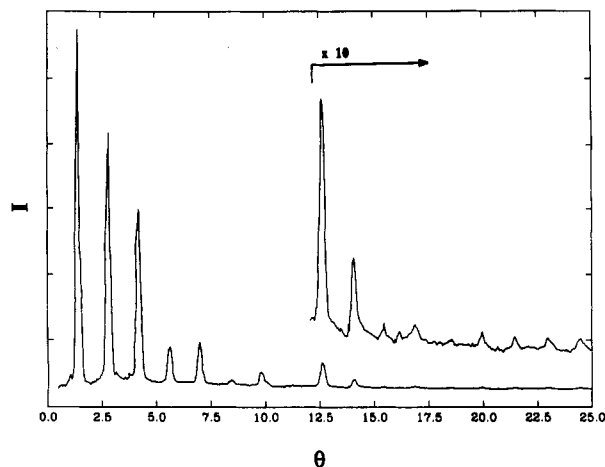


Figure 6. Low-angle X-ray reflection of Cd-[4]staffane-3-carboxylate. The substrate background has been subtracted.

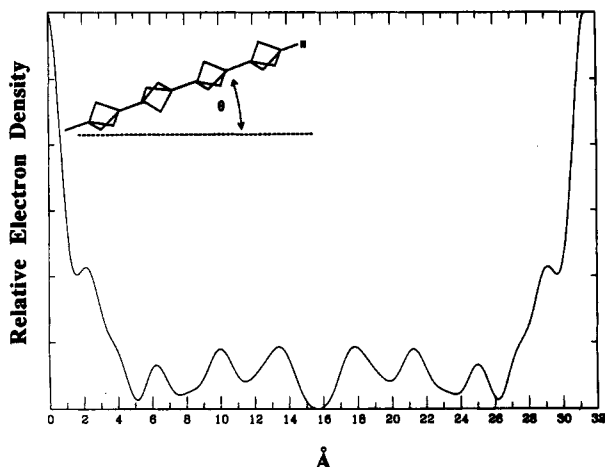


Figure 7. Projection of the unit cell electron densities onto the surface normal for Cd-[4]staffane-3-carboxylate.

of the film thickness by the less accurate ellipsometric method may be due to an error in the n_i assumed. The effect of such an error on the determination of the tilt angle would be small, because of its differential nature.

Accepting the X-ray values as the more accurate, and accepting a tilt of $17 \pm 5^\circ$, we can derive the effective length of a back-to-back arranged rod pair. This is 27.0 Å for Ca²⁺ 1[3], 33.6 Å for Ca²⁺ 1[4], and 32.8 Å for Cd²⁺ 1[4]. These values are quite reasonable and support our analysis, including the critically important assumption that the 1[3] and 1[4] carboxylates pack in the same way. Admittedly, the values to be expected are not very well defined in the absence of information on the details of the packing. If the rods in the two bilayers were antiparallel and coaxial, with the metal ion on the axis, one would expect an end-to-end length of about 37 Å for 1[4] salts from the single-crystal X-ray analysis of 1[2]¹⁷ and of the parent [*n*]staffanes,¹⁶ standard van der Waals radii for hydrogen, and ionic radii for Ca²⁺ or Cd²⁺. The observed value of 33–34 Å again suggests that interdigitation occurs at the interlayer contact planes.

The small difference between Ca²⁺ 1[4] and Cd²⁺ 1[4], apparent in both methods of measurement, seems to be real and may be due to differences in packing of the metal ions.

We next present the results of IR measurements on the multilayer assemblies, which provide an independent estimate of the tilt angle and its dependence on the nature of the counterion. Since they had to be performed on different substrates, the molecular orientation in the first

layer could be different, but this would not be likely to affect significantly the average value for the multilayer assembly.

IR Spectroscopy. General. A prerequisite for the use of IR spectroscopy for the characterization of L-B multilayers and monolayers is the knowledge of transition moment directions of the prominent vibrations in the individual constituent molecules. The IR transitions in the $[n]$ staffane skeleton^{14,16,21} as well as those in the carboxylate group are well understood. In the absence of perturbations by the counterion, transitions in the salts of $1[n]$ fall into four classes: (a) nondegenerate transitions polarized along the 3-fold symmetry axis of the $[n]$ staffane framework, such as the terminal CH stretch at about 2980 cm^{-1} , the CH_2 wag near 1215 cm^{-1} , and the symmetric CO_2 stretch near 1440 cm^{-1} ; (b) nondegenerate transitions polarized along the O...O direction of the CO_2^- group such as the antisymmetric CO stretch near 1535 cm^{-1} ; (c) nondegenerate transitions polarized perpendicular to the plane of the CO_2 group, which we have not observed; (d) doubly degenerate transitions perpendicular to the long molecular axis, such as CH_2 stretches near 2870 and 2905 cm^{-1} (the degeneracy is exact in the parent hydrocarbons and should be removed to a small degree in the presence of the carboxylate group at one of the termini, but this splitting is unobservably small). The only other IR peak in our spectra that is sufficiently intense to be easily measurable is located at 2970 cm^{-1} . It is known¹⁴ to be of mixed polarization due to band overlap and is thus not useful for the present purposes.

IR Intensities and Orientation Factors. As long as the substrates are optically inert, the samples optically uniaxial, and the IR transitions well separated in the spectra, a quantitative evaluation of the results is straightforward.²² These conditions are well fulfilled for the normal incidence measurements on Ge substrates, but the metal substrate used in the grazing angle reflectance measurements complicates matters.²³⁻²⁵ Since we observe no peak shifts and no enhanced reflections, we shall assume that the simple treatment is adequate to the first approximation even in this instance, i.e., that the effect of the metal surface is merely to suppress all absorption that would be due to that component of a transition moment that is parallel to the surface.

We use the electric dipole approximation and assume that the changes of sample polarizability and refractive index with wavelength are the same in the film and in isotropic powder. We introduce the usual definition of the orientation factor of the transition moment of the k th degenerate component of an n -fold degenerate i th vibration

$$K_{ik} = \langle \cos^2(ik, Z) \rangle \quad (1)$$

The pointed brackets indicate ensemble averaging and (ik, Z) is the angle between the transition moment of the k th component of i th vibration and the normal to the surface, Z .

We label the peak intensities of transition i measured in the L-B film at normal incidence A_i^N , those measured at grazing incidence A_i^G , and those measured in the

isotropic powder, A_i^{iso} . Then, transitions i and j can be characterized by the ratios Q_{ij}^N and Q_{ij}^G

$$Q_{ij}^N = A_i^{\text{iso}} A_j^N / A_j^{\text{iso}} A_i^N = (n/m) \sum_{k=1}^m (1 - K_{jk}) / \sum_{l=1}^n (1 - K_{il}) \quad (2)$$

$$Q_{ij}^G = A_i^{\text{iso}} A_j^G / A_j^{\text{iso}} A_i^G = (n/m) \sum_{k=1}^m K_{jk} / \sum_{l=1}^n K_{il} \quad (3)$$

We shall use the doubly degenerate CH_2 stretching vibration at 2905 cm^{-1} , which is of class d, as our reference vibration j , so that $m = 2$. The measured ratios will then be labeled $Q_{i,d}^N$ and $Q_{i,d}^G$.

Using α for the inclination of the $[n]$ staffane axis from the surface normal Z and defining the average inclination $\langle \alpha \rangle$ by $\cos^2 \langle \alpha \rangle = \langle \cos^2 \alpha \rangle$, we obtain

$$\sum_{k=1}^m (1 - K_{jk}) = 1 + \cos^2 \langle \alpha \rangle \quad (4)$$

$$\sum_{k=1}^m K_{jk} = \sin^2 \langle \alpha \rangle \quad (5)$$

for this vibration and all other vibrations of class d. For these vibrations, we therefore expect $Q_{d,d}^N = Q_{d,d}^G = 1$, and measurements on more than one of them merely provide a consistency check.

For vibrations of the other three classes, which are not degenerate, $n = 1$, and the subscript k is not needed

$$Q_{i,d}^N = (1 + \cos^2 \langle \alpha \rangle) / 2(1 - K_i) \quad (6)$$

$$Q_{i,d}^G = \sin^2 \langle \alpha \rangle / 2K_i \quad (7)$$

Now, $Q_{i,d}^N$ and $Q_{i,d}^G$ contain information on the average inclination angle $\langle \alpha \rangle$. The three classes of vibration differ in their values of K_i , which describe the average orientation of their transition moments relative to the surface normal.

For vibrations of class a

$$K_i = K_a = \cos^2 \langle \alpha \rangle \quad (8)$$

while for vibrations of classes b and c, K_i reflects the orientation of the CO_2^- group relative to the surface. If the O...O direction lies in the surface, we have $K_i = K_b = 0$ for a vibration of class b, polarized along O...O. Rotation of the OCO plane about the molecular long axis from this position by angle β yields

$$K_i = K_b = \sin^2 \langle \alpha \rangle \sin^2 \langle \beta \rangle \quad (9)$$

where $\sin^2 \langle \beta \rangle = \langle \sin^2 \beta \rangle$. When the OCO plane is perpendicular to the surface, $K_i = K_b = \sin^2 \langle \alpha \rangle$.

For a vibration of class c, $\sin^2 \beta$ would need to be replaced by $\cos^2 \beta$ in eq 9 for $K_i = K_c$, so that the results for O...O parallel to the surface and OCO perpendicular to the surface would be interchanged. However, we observe no vibrations of this class in our spectra.

Note that the statements about the K_i values for the transition moment directions hold only if the vibrations are those of the isolated molecule and are not affected significantly by the counterions. This is far more likely to hold for the 1215- cm^{-1} CH_2 (class a) than the 1440- cm^{-1} symmetric CO_2^- stretch (class a) and the 1535- cm^{-1} asymmetric CO_2^- stretch (class b). We shall, therefore, use the $Q_{a,d}^N$ and $Q_{a,d}^G$ values obtained from the intensity of the 1215- cm^{-1} vibration as our primary tool for the evaluation of the average tilt angle $\langle \alpha \rangle$. Substituting $K_i = K_a = \cos^2 \langle \alpha \rangle$ into eq 6 and 7, we obtain

(21) Obeng, Y. S.; Laing, M. E.; Friedli, A. C.; Yang, H. C.; Wang, D.; Thulstrup, E. W.; Bard, A. J.; Michl, J. *J. Am. Chem. Soc.*, in press.

(22) Michl, J.; Thulstrup, E. W. *Spectroscopy with Polarized Light. Solute Alignment by Photoselection, in Liquid Crystals, Polymers, and Membranes*; VCH Publishers: Deerfield Beach, FL, 1986.

(23) Allara, D. L.; Baca, A.; Pryde, C. A. *Macromolecules* 1978, 11, 1215.

(24) Umemura, J.; Kamata, T.; Kawai, T.; Takenaka, T. *J. Phys. Chem.* 1990, 94, 62.

(25) Swalen, J. D.; Rabolt, J. F. In *FTIR Application to Chemical Systems*; Ferraro, J. R., Basile, L. J., Eds.; Academic Press: New York, 1985; Chapter 7.

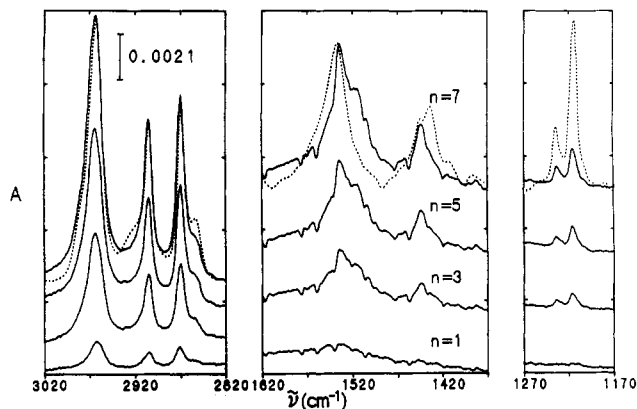


Figure 8. Normal incidence IR spectra of Cd-[4]staffane-3-carboxylate multilayer films on Ge. The number of bilayers is n . The dotted line shows the isotropic spectrum.

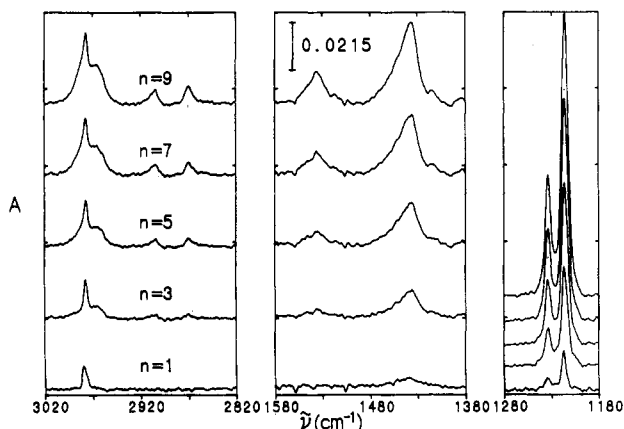


Figure 9. Grazing incidence IR spectra of Cd-[4]staffane-3-carboxylate multilayer films on Au-coated glass. The number of bilayers is n .

$$\langle \alpha \rangle = \tan^{-1} [1/(Q_{a,d}^N - 1/2)]^{1/2} \quad (10)$$

$$\langle \alpha \rangle = \tan^{-1} (2Q_{a,d}^G)^{1/2} \quad (11)$$

If the $Q_{a,d}^N$ and $Q_{a,d}^G$ values derived from the intensity of the 1440-cm^{-1} CO_2^- vibration agreed with that obtained from the 1215-cm^{-1} vibration, it would indicate that the symmetry of the CO_2^- substituent is not perturbed by the counterion, and one could then obtain the average rotation angle (β) of the carboxylate group from a combination of expressions 6 or 7, $i = b$, and (9–11).

IR Measurements on Cd^{2+} 1[4]. Both the normal incidence and the grazing incidence absorbances were proportional to the number of layers in the film, except for the first layer. Results of normal incidence measurements were independent of the state of polarization of the light and all attempts to detect a deviation from uniaxial behavior failed. Results for multilayer assemblies are shown in Figure 8 (normal incidence) and Figure 9 (grazing incidence). Results for a monolayer are shown in Figure 10.

In all cases, peaks appear at the same locations as in the isotropic spectrum, which is also shown in Figure 8, but their intensity distribution is very different. The large relative suppression of the 1215-cm^{-1} peak at the normal incidence and its relative enhancement at grazing incidence immediately demonstrate that the $[n]$ staffane rods are standing up on the surface. The effect is particularly striking for the monolayer: in Figure 10, the 1215-cm^{-1} peak is nearly absent at normal incidence (Ge substrate) and the 2870- and 2905-cm^{-1} peaks are not detectable at grazing incidence (Au substrate). The

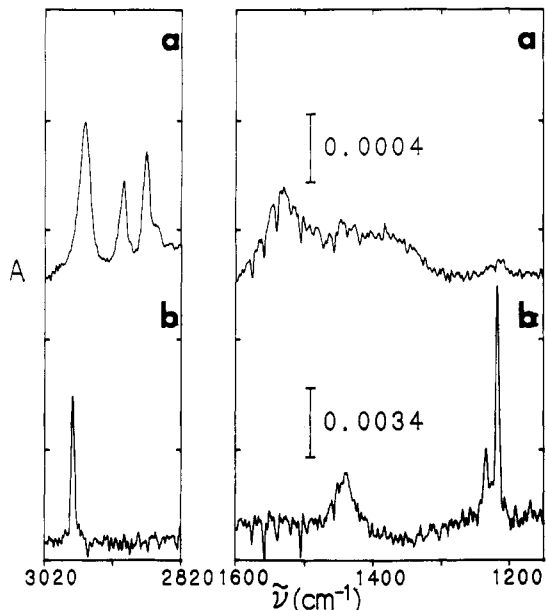


Figure 10. IR spectra of a Cd-[4]staffane-3-carboxylate monolayer: (a) normal incidence on Ge; (b) grazing incidence on Au-covered glass.

Table I. IR Intensity Ratios and the Average Tilt Angle (α) for Cd^{2+} 1[4]^a

no. of layers	$Q_{i,d}^N$ ^b				$\langle \alpha \rangle$ ^c	$Q_{i,d}^G$ ^d				$\langle \alpha \rangle$ ^e
	1215	1440	1535	2870		1215	1440	1535	2870	
1	4.5	∞	1.2	0.86	27	0.0	0.0			0
3	4.0	1.5	1.4	1.0	28	0.059	0.097	0.54	1.1	19
5	3.9	1.6	1.3	0.98	28	0.059	0.10	0.56	1.1	19
7	4.1	1.5	1.1	0.88	28	0.057	0.098	0.45	1.1	19
9						0.062	0.097	0.45	1.0	19

^a The 2905-cm^{-1} vibration serves as the standard vibration j . The error limits shown are $\pm 2^\circ$ for the multilayers and $\pm 10^\circ$ for the monolayer and reflect the estimated accuracy with which integrated peak intensities can be measured but no other sources of error. ^b Equation 2, germanium substrate. ^c Tilt angle in degrees calculated from $Q_{a,d}^N$. ^d Equation 3, gold substrate. ^e Tilt angle in degrees calculated from $Q_{a,d}^G$.

relative intensity of the single terminal CH stretch near 2980-cm^{-1} in the grazing incidence spectrum of Figure 10 contrasts eloquently with the absence of any intensity for the stretching vibrations of the 24 C–H bonds in the CH_2 groups. In contrast, in the isotropic spectrum, the peak due to the terminal CH stretch is completely buried under the tail of the CH_2 stretching peaks.

Clearly, on the gold substrate, the $[n]$ staffane rods in the monolayer are lined up essentially exactly (within 10°) perpendicular to the surface. On the germanium substrate, the average tilt is clearly larger. Comparison with Figures 8 and 9 demonstrates that in multilayer assemblies the tilt angle also differs from zero significantly.

Results of a quantitative evaluation of the ratios $Q_{i,d}^N$ and $Q_{i,d}^G$ are collected in Table I, which also lists the average tilt angles (α). The expected relation $Q_{a,d}^N = Q_{a,d}^G = 1$ is fulfilled well. The tilt angles in the multilayers derived from the grazing incidence measurements ($22 \pm 2^\circ$) agree with those derived from ellipsometry ($15\text{--}35^\circ$) and X-ray deflection ($12\text{--}21^\circ$), those derived from normal incidence measurements deviate systematically toward somewhat larger values ($28 \pm 2^\circ$). We believe that the larger average tilt angle on the Ge surface is due to its relative roughness and does not necessarily reflect any intrinsic property of the L–B film on germanium.

The intensity ratios for the vibrations of the CO_2^- group do not follow the expected pattern. In particular, the

symmetric CO_2^- stretch at 1440 cm^{-1} , which should have the same $Q_{a,d}^N$ and $Q_{a,d}^G$ values as the CH_2 wag at 1215 cm^{-1} , has quite different values and it is obvious that its average transition moment direction is perturbed by the counterion and does not point along the $[n]$ staffane axis. Under these circumstances, it is pointless to try to interpret the significance of the intensity ratios for both the CO_2^- vibrations at the present time. Since there are two molecules of 1[4] for every Cd^{2+} cation, it is quite likely that there are two or more distinct carboxylate sites and that the observations reflect a complicated average.

Conclusions

Salts of $[n]$ staffane-3-carboxylic acids, $n = 3$ and 4, form stable L-B films. In a monolayer, the $[n]$ staffane rods stand perpendicular to the surface on a gold substrate,

and probably on germanium as well. In a multilayer, they pack at a tilt angle of about 20° , very similar to those found in the single crystal of the $[n]$ staffane hydrocarbons, $n = 3$ and 4.

Acknowledgment. We are grateful to the National Science Foundation for support (DMR 8807701 and CHE 8901450) and for an equipment grant (CHE-9022151) and to the Robert A. Welch Foundation (F-1068) for support. We are grateful to Professor H. Steinfink and Dr. S. Swinnea for use of their equipment and help with the measurement of the X-ray diffraction patterns.

Registry No. 1[4], 137335-11-6; Ca-1[3], 143733-08-8; Ca-1[4], 143733-09-9; Cd-1[4], 143733-10-2; Ge, 7440-56-4; Si, 7440-21-3; Au, 7440-57-5.